Modelling an NMR probe for Magnetometry

G. Boero, D. Schlaefli, P. A. Besse and R.S. Popovic

Swiss Federal Institute of Technology, EPFL-DMT-IMS, Room BM-3-110
CH-1015 Lausanne, Switzerland, giovanni.boero@epfl.ch

ABSTRACT

A model of an NMR magnetometer probe head, based on the Bloch equations, has been developed and implemented in a C-program. The program permits to simulate pulsed and continuous wave NMR experiments with a probe head consisting of a single coil, for excitation and detection of the NMR signal, and of a resonating sample. Compare to existing programs, it is well adapted to the presence of a non-uniform and frequency variable RF magnetic field. The model has been successfully tested by comparison with experimental results.

Keywords: NMR magnetometer; Integrated NMR sensor, Bloch equations; Microcoils.

INTRODUCTION

The nuclear magnetic resonance (NMR) phenomenon is widely used for high precision measurements of static magnetic fields [1]. A precision better then 5 ppm is achieved for magnetic fields higher then 0.1 T by commercial instruments (e.g., PT2025, Metrolab). A precision of 0.01 ppm at 1.7 T has been obtained recently by a non-commercial apparatus [2]. Special techniques (e.g. flowing water [3] dynamic nuclear polarization [4] and optical pumping [5]) permits to extend the NMR method to the measurement of the earth magnetic field, with a precision of the order of 1ppm.

We are developing an integrated NMR magnetometer [6] for measuring static magnetic fields higher then 0.1 T with a precision of the order of 1 ppm. It basically consists of a planar coil (diameter of about 1mm) directly integrated on a silicon substrate (surface of about 10 mm^2), where the CMOS electronics for signal detection and amplification is also integrated (figure 1). A sample of a resonating material (volume of about 1 mm^3), is placed over the planar coil. Thanks to the use of smaller samples the sensor will be able to measure an order of magnitude less uniform fields with an order of magnitude better spatial resolution with respect to the state-of-the-art NMR magnetometers. Since the sample volume is reduced, the NMR signal induced in the coil is more than an order of magnitude smaller with respect to that of conventional apparatus. For this reason the probe head (coil and sample), the excitation parameters and the detection electronics must be carefully optimised.

Simulation programs [7, 8] of NMR systems have been recently developed, in particular for NMR imaging. None of these programs is well adapted to our problem. In particular they do not take into account the non-uniform and frequency variable RF field produced by our planar coils with a continuous wave excitation.

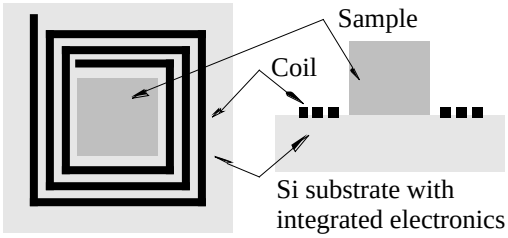

Figure 1: The integrated NMR magnetometer probe.

In this paper we describe a model of the NMR probe head. We have devoted our attention to the calculation of the induced voltage across the planar coil by the NMR effect in the sample. Our model permits to study the effects of the coil and sample geometry, of the sample physical properties and of the static and RF magnetic field excitations on the amplitude and shape of the NMR signal. We also present some experimental results to show the good agreement with this modelization.

THE MODEL

In this section we describe the basic concepts and hypothesis of the model. In particular, we show the method employed to compute the induced electromotive force across the coil due to the NMR effect in the sample.

Let us consider a small portion dV_s of a sample S containing nuclei with non-zero magnetic moment placed in the point $\mathbf{r}_s$. The effect of an applied magnetic field $\mathbf{B}(t,\mathbf{r}_s)$ is to produce a nuclear magnetization $\mathbf{M}(t,\mathbf{r}_s)$. If a conducting coil C is placed in proximity of the sample the magnetization vector $\mathbf{M}(t,\mathbf{r}_s)$ will induce an electromotive force $d\zeta(t,\mathbf{r}_s)$ in the coil C (figure 2).

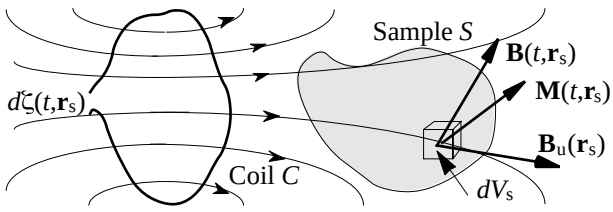

Figure 2: The nuclear magnetization $\mathbf{M}(t,\mathbf{r}_s)$ induces a electromotive force $d\zeta(t,\mathbf{r}_s)$ in the coil C.

Using the principle of reciprocity [9] it may be shown that the induced electromotive force is given by:

$$d\zeta(t,\mathbf{r}_s) = -\frac{d}{dt}\left(\mathbf{M}(t,\mathbf{r}_s)\ \mathbf{B}_u(\mathbf{r}_s)\right)dV_s \qquad (1)$$

where $\mathbf{B}_u(\mathbf{r}_s)$ is the magnetic field at position $\mathbf{r}_s$ produced by a unit current passing carried by the coil *C*.

In a NMR experiment the applied magnetic field $\mathbf{B}(t,\mathbf{r}_s)$ is usually the superposition of a static magnetic field $\mathbf{B}_0(\mathbf{r}_s)$ and of the much smaller RF magnetic field $\mathbf{B}_{rf}(t,\mathbf{r}_s)$:

$$\mathbf{B}(t,\mathbf{r}_s) = \mathbf{B}_0(\mathbf{r}_s) + \mathbf{B}_{rf}(t,\mathbf{r}_s). \qquad (2)$$

If the applied RF magnetic field $\mathbf{B}_{rf}(t,\mathbf{r}_s)$ has a frequency $\omega(t)\approx\omega_0\equiv-\gamma B_0$, the nuclear magnetization vector $\mathbf{M}(t,\mathbf{r}_s)$ can be computed by means of the Bloch phenomenological equation [10]:

$$\frac{d\mathbf{M}}{dt} = \gamma\mathbf{M}\times\mathbf{B} - \frac{M_x\mathbf{i} + M_y\mathbf{j}}{T_2} - \frac{M_z - M_o}{T_1}\mathbf{k} \qquad (3)$$

where $(\mathbf{i},\mathbf{j},\mathbf{k})$ are the unit vectors of a fixed (respect to the coil and the sample) frame of reference. $\mathbf{k}$ is defined by the $\mathbf{B}_0(\mathbf{r}_s)$ direction, T_1 is the spin-lattice relaxation time, T_2 is the spin-spin relaxation time and γ is the gyromagnetic ratio of the nuclei in the sample *S*. The equilibrium nuclear magnetization M_0 is the nuclear magnetization when $\mathbf{B}_{rf}(t,\mathbf{r}_s)=0$:

$$\mathbf{M}_0(\mathbf{r}_s) = M_0(\mathbf{r}_s)\mathbf{k} = \frac{\chi_0}{\mu_0}B_0(\mathbf{r}_s)\mathbf{k}, \qquad (4)$$

where χ_0 is the static nuclear susceptibility [10].

Usually the RF magnetic field $\mathbf{B}_{rf}(t,\mathbf{r}_s)$ is linearly polarized. We can take the $\mathbf{j}$ unit vector so that the vector $\mathbf{B}_{rf}(t,\mathbf{r}_s)$ is in the plane *xz*:

$$\mathbf{B}_{rf}(t,\mathbf{r}_s) = 2B_{1x}(\mathbf{r}_s)\cos\alpha(t)\mathbf{i} + 2B_{1z}(\mathbf{r}_s)\cos\alpha(t)\mathbf{k} \qquad (5)$$

where:

$$\alpha(t) = \int_0^t \omega(t)dt. \qquad (6)$$

The component of the RF magnetic field polarized along $\mathbf{i}$ can be considered as a superposition of two fields circularly polarized rotating in opposite direction with angular velocity $\omega(t)$. It can be shown, by means of the energy and angular momentum conservation laws in the interactions between photons and nuclei, that the field rotating in the direction opposite to the Larmor precession ($\mathbf{k}$ if $\gamma>0$) as well as the RF field component parallel to the static magnetic field $B_0\mathbf{k}$ can be neglected in the evaluation of the motion of the magnetization vector $\mathbf{M}(t,\mathbf{r}_s)$.

The equation (3), in a frame rotating around $\mathbf{k}$ at the frequency $\omega=\omega(t)\mathbf{k}$, becomes:

$$\frac{d\mathbf{M}}{dt} = \gamma\mathbf{M}\times\mathbf{B}_{\text{eff}} - \frac{M_x'\mathbf{i}' + M_y'\mathbf{j}'}{T_2} - \frac{M_z' - M_o'}{T_1}\mathbf{k}' \qquad (7)$$

where:

$$\mathbf{B}_{\text{eff}} = \left(B_0 + \frac{\omega(t)}{\gamma}\right)\mathbf{k}' + B_{1x}\mathbf{i}' \qquad (8)$$

is called the effective static field in the rotating frame, $(\mathbf{i}',\mathbf{j}',\mathbf{k}')$ are the unit vectors of the rotating frame and M_x', M_y', M_z' are the components of $\mathbf{M}(t,\mathbf{r}_s)$ in the rotating frame.

From the previous equation we have that:

$$\begin{aligned}
\frac{dM_x'}{dt} &= -\frac{M_x'}{T_2} + \Delta\omega M_y',\\
\frac{dM_y'}{dt} &= -\Delta\omega M_x' - \frac{M_y'}{T_2} - \omega_1 M_z',\\
\frac{dM_z'}{dt} &= \omega_1 M_y' - \frac{M_z' - M_o}{T_1},
\end{aligned} \qquad (9)$$

where $\omega_0=-\gamma B_0$, $\omega_1=-\gamma B_{1x}$ and $\Delta\omega=\omega(t)-\omega_0$.

The components of $\mathbf{M}(t,\mathbf{r}_s)$ in the fixed frame are:

$$\begin{aligned}
M_x &= M_x'\cos\alpha(t) - M_y'\sin\alpha(t),\\
M_y &= M_x'\sin\alpha(t) + M_y'\cos\alpha(t),\\
M_z &= M_z'.
\end{aligned} \qquad (10)$$

If the same coil is used for detecting the NMR signal $d\zeta(t,\mathbf{r}_s)$ and to produce the RF magnetic field $\mathbf{B}_{rf}(t,\mathbf{r}_s)$ we have that $B_{uy}(\mathbf{r}_s)=0$ and then, from (1), (9) and (10):

$$\begin{aligned}
d\zeta(t,\mathbf{r}_s) = \Big[& B_{ux}(\mathbf{r}_s)\left(\frac{M_x'}{T_2} + M_y'\omega_0\right)\cos\alpha(t) + \\
& + \left(-\frac{M_y'}{T_2} + M_x'\omega_0 - \omega_1 M_z'\right)\sin\alpha(t)\Big] + \\
& + B_{uz}(\mathbf{r}_s)\left(\frac{M_z' - M_0}{T_2} - \omega_1 M_y'\right)dV_s.
\end{aligned} \qquad (11)$$

In this equation we can distinguish the absorption component (in phase with respect to the excitation current that produce the RF magnetic field $\mathbf{B}_{rf}(t,\mathbf{r}_s)$) and the dispersion component (90º out of phase with respect to the excitation current), both at a frequency close to ω_0, and a small component at frequency much smaller than ω_0.

The total electromotive force induced in the coil by the whole sample *S* is then given by:

$$\zeta(t) = \int_{V_S} d\zeta(t,\mathbf{r}_s). \qquad (12)$$

IMPLEMENTATION OF THE MODEL

In the previous section we have described the way adopted to compute the induced electromotive force across the coil. In this section we want to spend a few words on the C-program that execute the computation.

The program has an input file that contains all the parameters for the simulation. These parameters, in particular, define:

a) the sample and coil geometry.
b) the sample physical properties γ, χ_0, T_1 and T_2.
c) the static magnetic field distribution in the sample $\mathbf{B}_0(\mathbf{r}_s)$.
d) the excitation current frequency and amplitude, both as a function of time.

Input file parameters

The sample geometry and position with respect to the coil is specified together with the number of representative points. The sample dimensions and position are measured with an accuracy of about 10%. The coil geometry is specified together with the wire width and thickness and the number of representative points. The coil dimensions are measured with an accuracy better then 10%.

The sample physical parameters are collected from literature or measured in our laboratory. The gyromagnetic ratio γ is a property of each nucleus in given state. It is measured for all the nuclei with an absolute accuracy of the order of 1 ppm. The static nuclear magnetization χ_0 can be estimated by means of the Curie like equation [10]:

$$\chi_0 = N \frac{\gamma^2 \hbar^2 I(I+1)}{3K_B T} \mu_0 \qquad (13)$$

where I is the spin of the nuclei, N is the density of nuclei and T is the temperature of the sample. The density of nuclei can be estimated by means of the density and of the chemical composition of the sample. With our samples we have estimate an error in the evaluation of the spin density smaller then 10%. The overall accuracy in the evaluation of χ_0 can be reasonably considered limited only by this incertitude.

The relaxation times T_1 and T_2 are dependent on temperature, magnetic field intensity, presence of paramagnetic impurities and many others factors. Due to the difficulty to compute these parameters theoretically, we have measured T_1 and T_2. T_1 is measured with a $(180°-\tau_i\text{-}90°)_i$ pulse sequence and T_2 by measuring the resonance line-width in a sufficiently uniform static magnetic field [10].

The static magnetic field $\mathbf{B}_0$ is specified by a uniform field and a gradient tensor. Its value can be measured with an accuracy of the order of 5 ppm by means of an NMR magnetometer.

The excitation current can be of constant amplitude but variable frequency (continuous wave mode) or a sequence of pulses of any amplitude, length and frequency (pulsed mode). Its value can be evaluated with an accuracy of the order of 20%.

Program description

The program firstly generates (pseudo-randomly within the defined coil and sample volumes) the representative points of the coil and of the sample. Secondly it computes the magnetic field generated by a unit current flowing into the coil C, the unitary field $\mathbf{B}_u(\mathbf{r}_s)$, in each representative point of the sample S by means of the Biot-Savart law. The RF magnetic field $\mathbf{B}_{rf}(t,\mathbf{r}_s)$ is obtained by multiplying the unitary field $\mathbf{B}_u(\mathbf{r}_s)$ by the excitation current. Subsequently the program computes the time evolution of the magnetization vector $\mathbf{M}(t, \mathbf{r}_s)$ in each point of the sample by means of the Bloch equations (9). The Bloch equations forms a system of three coupled first order differential equations. The numerical solution of such a system is obtained by means of the Runge-Kutta 4th order method. Finally, using equation (11) and (12), the program computes the induced electromotive force across the coil.

The time step for this numerical solution must be small compared to the period of the motion of the magnetization vector in the rotating frame ($\sim 1/(\omega_1+\Delta\omega)$). This shows the advantage of solving the Bloch equations in the rotating frame: in the fixed frame the period of the motion of the magnetization is of the order of $(1/\omega_0)$. A further reduction of the time step is necessary because the excitation current can be, in principle, any function of time with the only restriction that it should produce an RF magnetic field $\mathbf{B}_{rf}(t,\mathbf{r}_s)$ of amplitude small compared with the static magnetic field $\mathbf{B}_0(\mathbf{r}_s)$ and of frequency $\omega(t)$ close to ω_0 ($\Delta\omega << \omega_0$). This means that the rotating frame (as well as the magnetization vector in this frame) rotates at variable angular frequency. In order to avoid divergence problems, it is sufficient to choose a time step so that the variation of the period of oscillation of the excitation current during a time equivalent to the time step is small respect to the time step itself.

COMPARISON WITH EXPERIMENTS

In this section we present a comparison between simulation and experimental results obtained with a probe head consisting of a planar spiral (circular) coil and of a cylindrical sample, both of linear dimension of a few millimeters. The natural rubber sample (90% cis-polyisoprene) has a ^{1}H spin density $N=6\cdot10^{28}/m^3$. At 295 K and 1.4 T, we have measured T_2=0.5ms and T_1=70ms. From equation (13) we have $\chi_0=3.9\cdot10^{-9}$. The wiggles (fig. 3) and the saturation phenomena (fig. 4) as well as the effect of the rate of variation of the excitation frequency (fig. 5) are well predicted [10]. No fitting parameters are necessary to match the experimental results.

We have estimated an error in the amplitude of the excitation current and of the signal amplitude of about 20%. Taking into account that some parameter of the model are known with an accuracy of the order of 10% we believe that the agreement between simulation and experimental results is satisfactory.

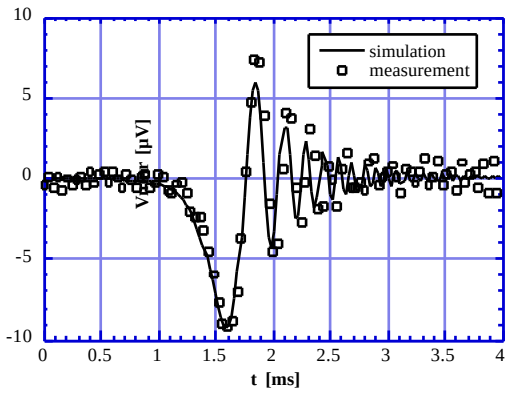

Figure 3: ^{1}H-NMR absorption signal *vs* time. Sample: natural rubber (radius 2.3mm, height 1.5mm, T_1=70ms, T_2=0.5ms). Planar coil: Cu on a PCB substrate (external diameter 5.0mm, 8turns, pitch 200µm, wire width 100µm, wire thick. 40µm). B_0=1.4T. Excitation: cw (coil current 3mA, central freq. 59.978MHz, sweep freq. 60Hz, sweep width 25kHz).

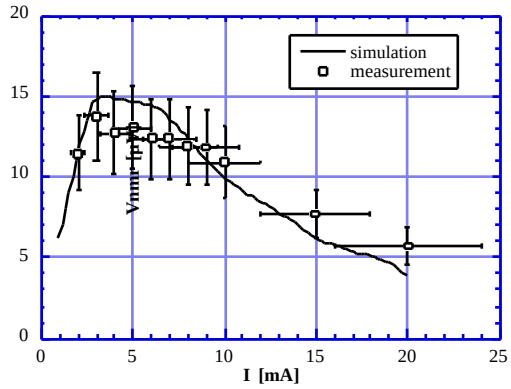

Figure 4: ^{1}H-NMR absorption signal amplitude *vs* coil current amplitude. Same condition as in fig. 3 but sweep freq. 20Hz. The error bars are of 20% for both current and NMR signal.

DISCUSSION AND CONCLUSIONS

In this paper we have described a way of computing the NMR signal by means of the Bloch equation. Our approach is neither more sophisticated nor general compared to other simulation programs in the field of NMR imaging based on the Bloch equation, but is the only one, at the best of our knowledge, well adapted to the presence of a non-uniform and frequency variable RF magnetic field.

The agreement between simulation and experimental results, in the case of natural rubber at room temperature and high magnetic fields, is good enough for our optimization purposes. Nevertheless, since the use of the Bloch equation for solid samples is always questionable, the applicability of the model to others solid samples or in other experimental conditions must be carefully evaluated.

The program will soon permit the simulation of a probe with a detection coil separated from the excitation coil. Since no additional hypothesis are needed we aspect a good behaviour also in this configuration. Moreover, it will be coupled to a program for signal-to-noise ratio optimization, that take into account the coil resistance, the parasitic effects of the coil substrate and the detection electronics.

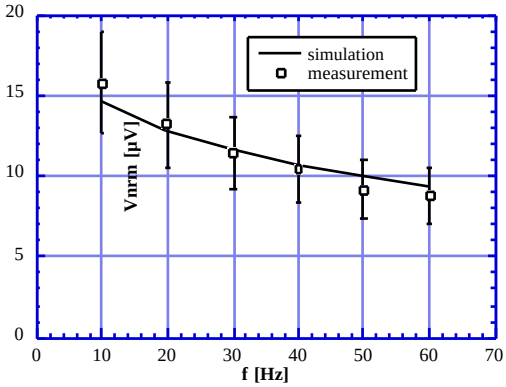

Figure 5: ^{1}H-NMR absorption signal amplitude *vs* sweep frequency. Same condition as in fig. 3. The error bars are of 20% for the NMR signal. The sweep frequency is known with an error of less than 1%.

ACKNOWLEDGEMENTS

This work has been partially supported by the Swiss priority program MINAST 3.03.

REFERENCES

[1] K. Borer and G. Fremont, *Nuclear Instruments and Methods in Physics Research*, 154, 61-82, 1978.
[2] R. Prigl, U. Haeberlen, K. Jungmann, G. zu Putlitz, and P. von Walter, *Nuclear Instruments and Methods in Physics Research A*, 374, 118-126, 1996.
[3] B. C. Woo, C. G. Kim, P. G. Park, C. S. Kim, and V. Y. Shifrin, *IEEE Transactions on magnetics*, 33, 4345-4348, 1997.
[4] N. Kernevez and H. Glénat, *IEEE Transactions on magnetics*, 27, 5402-5404, 1991.
[5] N. Kernevez, D. Duret, M. Moussavi, and J. M. Leger, *IEEE transactions on magnetics*, 28, 3054-3059, 1992.
[6] G. Boero, C. de Raad Iseli, P. A. Besse, and R. S. Popovic, *Sensors and Actuators A*, vol. 67, 18-23, 1998.
[7] A. R. Brenner, J. Kürsch, and T. G. Noll, *Magma*, 5, 129-138, 1997.
[8] Y. Taniguchi, C. Nakaya, Y. Bito, and E. Yamamoto, *Systems and computers in Japan*, 26, 54-62, 1995.
[9] D. I. Hoult and R. E. Richards, *Journal of magnetic resonance*, 24, 71-85, 1976.
[10] A. Abragam, *Principles of nuclear magnetism*, Oxford University Press Inc., 35-53, 1961.